Mirror electrode for laser initiated discharge channels

R. M. Gilgenbach and L. D. Horton

The University of Michigan, Department of Nuclear Engineering, Ann Arbor, Michigan 48109

(Received 4 October 1982; accepted for publication 6 December 1983)

A reflecting waxicon has been demonstrated to generate long, smooth, CO_2 laser induced breakdown plasmas in atmospheric pressure gases including nitrogen, argon, and air. A waxicon or compound axicon is a mirror consisting of two concentric cones which form a *W*-shaped cross section. The protruding central cone of the waxicon also functions as an electrode for laser guided electrical discharges. In contrast to conventional mirrors, this waxicon design produces nearly uniform laser intensity in a fixed length of breakdown plasma. The length of the laser induced breakdown plasma has been measured as a function of incident laser power and agrees well with predictions of a ray tracing code.

PACS numbers: 52.50.Jm, 52.80.Dy, 51.50. + v, 84.70. + p

INTRODUCTION

Recently, laser initiated discharge channels[1-4] have found important applications in electron and light ion beam transport systems for inertial confinement fusion reactors.[5-12] In order to generate these channels, high-voltage electrical discharges have been guided by long chains of laser induced breakdown plasma in atmospheric pressure gas[1-4,8,12] or reduced density gas.[9,10] Other applications of laser guided electrical discharges include a new technique for materials processing[13] and reproducible artificial lightning.

There exist several disadvantages to conventional lenses and mirrors concerning the generation of these laser induced breakdown plasmas by means of TEA CO_2 lasers using confocal, unstable resonators. First, the laser beam cannot propagate downstream through the overdense breakdown plasma, resulting in nonuniform laser energy deposition.[14,15] (The retractable focus has been studied by Weyl as a means of alleviating the overdense plasma cutoff.[16]) Second, the focused laser intensity varies strongly in the axial direction and an annular beam generates off axis breakdown. These sources of nonuniform energy deposition in the breakdown plasma could introduce initial hydrodynamic perturbations in the channel.[17]

The waxicon provides a focusing system which compacts the annular laser beam and, in the design discussed here, also has the advantage that downstream rays do not undergo the overdense plasma cutoff. Another unique feature of this waxicon for laser initiated plasma channels is that the focused laser intensity is relatively constant in the axial direction over a designated channel length. This waxicon design is useful for laser guided electrical discharges, since the design length of breakdown plasma begins at the tip of the center cone, which also functions as the discharge electrode.

I. WAXICON DESIGN AND EXPERIMENTAL CONFIGURATION

This waxicon was designed to generate 10- to 15-cm lengths of CO_2 laser induced breakdown plasma in atmospheric pressure gases. Our previous experiments[8] have demonstrated that laser guided electrical discharges with lengths of 6 cm or greater exhibit similar channel radius and onset times for turbulent convective mixing compared to the 0.5- to 2-m channels studied at the Naval Research Labs.[4] Another design feature of this waxicon is that the center cone must protrude in order to function as an electrode.

A cross-sectional view of the device is depicted in Fig. 1(a). Waxicons have typically been used to convert annular beams to collimated, solid beams.[18-19] For a linear waxicon, collimation can be accomplished by a symmetric design with

$$\phi_1 = \phi_2 = 45°,$$

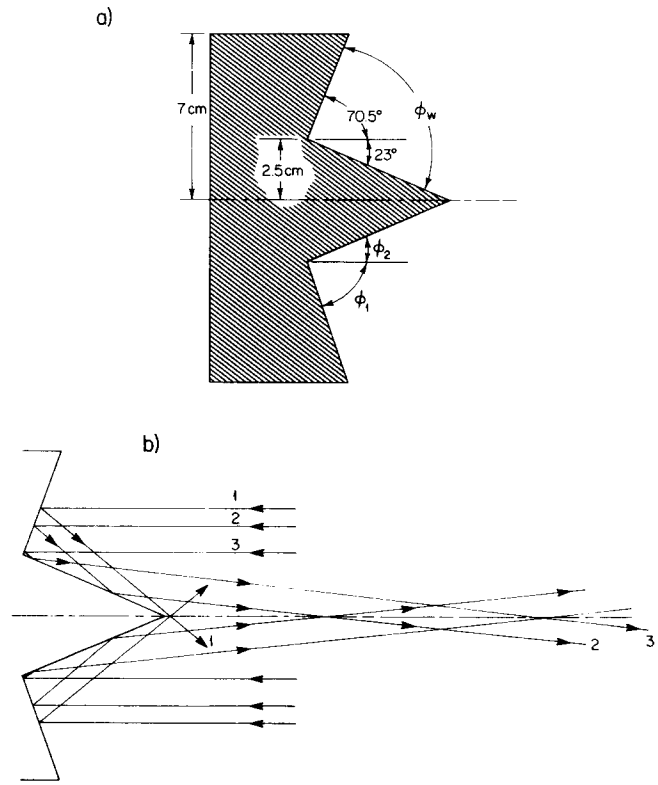

FIG. 1. (a) Cutaway view of the waxicon design, (b) ray diagram illustrating region of overlap for the CO_2 laser beam.

 0034-6748/84/040503-05$01.30

where the angles are defined in Fig. 1(a). However, by increasing the total angle ϕ_w, to a value greater than 90°, the beam overlaps into a quasi-line-focus over a chosen length, as depicted in the ray diagram of Fig. 1(b). (Note from this diagram that the downstream rays labeled 2 and 3 do not pass through the overdense laser induced breakdown plasma which occurs along the axis.) The angle θ, at which the ray crosses the axis is given by

$$\theta = 2\phi_w - 180^\circ .$$

Thus, for the typical waxicon design ($\phi_w = 90^\circ$) the exiting beam is collimated. For generating the desired laser induced breakdown lengths with our available peak power level the angle ϕ_w was chosen as 93.5°. The angles, ϕ_1 and ϕ_2, were chosen so that the outermost part of the elongated annular beam [ray 1 in Fig. 1(b)] would cross the axis directly in front of the inner waxicon cone (electrode) tip to ensure breakdown and subsequent electrical discharge guidance to this electrode.

Another design constraint upon this device concerned the use of the waxicon as an electrode. This required that the central cone protrude sufficiently from the waxicon so that the high-voltage electrical discharge would not arc to the outer edges of the device. To satisfy this condition ϕ_1 must be greater than ϕ_2. The ray tracing results presented in the next section show that these objectives were met in the chosen design.

The waxicon was fabricated from a solid bar of brass on a standard lathe. Polishing was performed on the lathe with a succession of fine sandpaper (400 and 600 grit), followed by optical polishing compound (#500 and #1000). The resultant surface had a finish which was sufficient to perform alignment with a helium–neon laser expanded through the unstable resonator of the CO_2 laser.

Configuration of the waxicon–electrode in the laser guided discharge experiment is illustrated in Fig. 2. The waxicon was electrically isolated from its supports and connected to the discharge circuitry by braided cable. Of the measured CO_2 laser energy, 60% was in a 40-ns (FWHM) triangular pulse with the remainder in a low-intensity tail. Incident intensity was controlled by means of a propylene absorption cell. The spark gap switch was triggered 0.4 μs after the CO_2 laser pulse in these experiments. For the 30-kV capacitor charging voltage the discharge current was 10 kA with a 2.5-μs ringing period and a $1/e$ decay time of 11 μs. The laser induced plasma and discharge channel dynamics were characterized by a ruby laser schlieren diagnostic which utilized a pinhole aperture to obtain two-dimensional spatial resolution. Adjustment of the relative delay between the CO_2 laser pulse and the (50 ns) ruby laser pulse permitted a study of the temporal evolution of laser induced breakdown and laser guided discharges.

Some optically induced damage to the cone tip was observed in these experiments. Although this damage and the damage caused by discharges did not measurably degrade the waxicon performance during our experiments, this does represent a disadvantage of this design. The center cone may easily be repolished on the lathe. An improved waxicon design has a removable center cone which can be replaced after damage impairs the optical properties.

II. RAY TRACING MODEL

A ray tracing program was developed which calculates power densities on the surface of the waxicon and along the z axis off the tip of the waxicon. With this code we have modeled this waxicon design and predicted the length of laser induced breakdown plasma for different peak laser powers. The model uses geometrical optics to trace the paths of a cylindrical array of points on the original CO_2 laser profile. For this study, a burn pattern on thermal paper was used to measure the shape of the incident beam (Fig. 2). Using the outer and inner dimensions of this pattern and a given number of mesh lines, the model calculates whether or not each

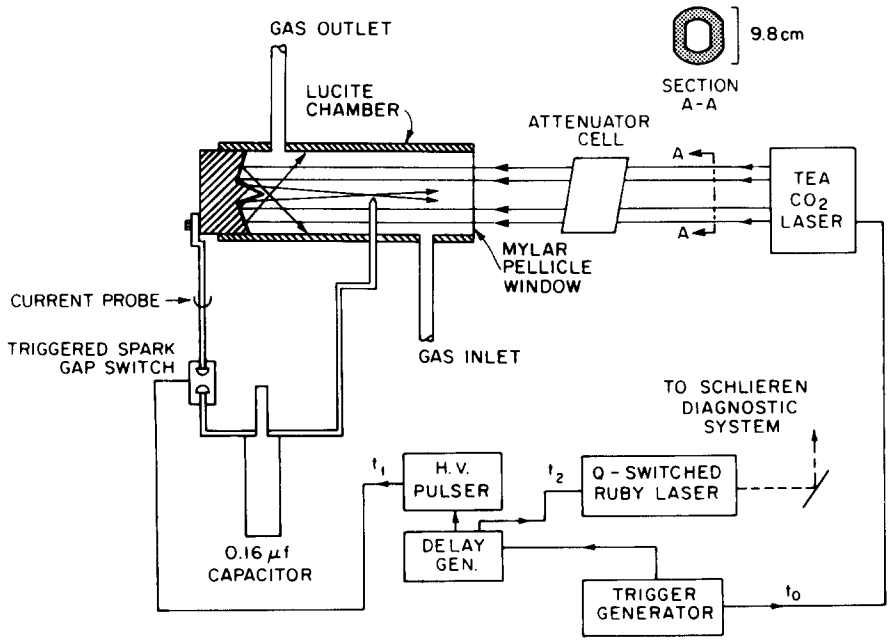

FIG. 2. Experimental configuration illustrating waxicon–electrode placement.

area bounded by its four surrounding mesh points is in or out of the CO_2 laser beam. No account was taken in the original model for energy profiles within the beam although this would be a simple programming addition. The actual ray tracing part of the program works from the inside of the incident beam out. Two types of rays must be considered here. As can be seen in Fig. 1(b) the rays traced by each ring in the mesh can reflect once or twice off the waxicon surface. Since we were interested in surface power densities on the inner cone of the waxicon, the position at which the doubly reflected rays make their second reflection was calculated as well as the position at which both classes of rays cross the z axis. Surface power densities as a function of r and θ are then calculated using the peak power of the CO_2 laser. For a perfect waxicon the reflected energy profile reaches a line focus limited only by the diffraction spot size of the beam. Note that this spot size is a function not only of the wavelength of the incident radiation but also of the mirror. Thus, the diffraction limit would be different for the singly and doubly reflected rays. However, since our waxicon was turned on a standard lathe, the spot size of the line focus is limited by imperfections in machining. In our model a spot radius is assumed and laser energy is averaged over the resulting tube around the z axis. This radius was found by examining schlieren photographs of newly formed breakdown plasmas ($\sim$ 100 ns after the peak CO_2 laser power level is reached). In this study a 0.25-mm radius was used. Our model calculates an effective power density (W/cm^2) by multiplying the averaged energy density (J/cm^3) by the speed of light and the cosine of the angle between the Poynting vector and the axis of the waxicon.

A typical plot of power density versus axial distance is shown in Fig. 3. One of the important characteristics of the waxicon for the generation of uniform plasma channels is the nearly constant intensity plateau over a distance of 10 cm (from 2 to 12 cm in Fig. 3). Note the high-intensity region at 0–1.5 cm, which corresponds to the region where both singly and doubly reflected rays are crossing the axis. The final shelf at 12–14.5 cm is a result of the shape of the unstable resonator mirrors in the CO_2 laser (Fig. 2). The front mirror is not circular but rather has straight sides which are closer to the center of the annulus. As a result, energy deposition from the top and bottom part of the incident beam cuts off at 12 cm while the sides contribute out as far as 14.5 cm. This predicted intensity distribution has been compared to the experimental results described below.

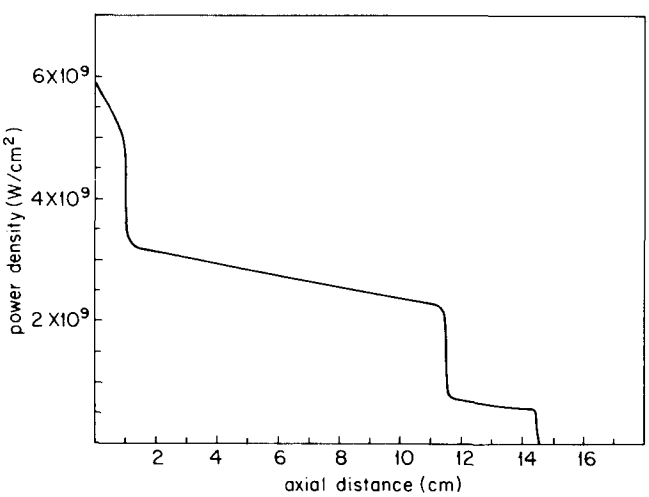

FIG. 3. Power density on axis as a function of distance from the tip of the waxicon for a peak incident laser power of 0.18 GW.

III. EXPERIMENTAL RESULTS

Schlieren photographs are given in Fig. 4 for laser induced argon breakdown by means of the waxicon focus. The photo in Fig. 4(a), taken 0.3 μs after the CO_2 laser pulse, shows that the long, narrow, breakdown plasma occurs along the line focus which extends out from the tip of the inner waxicon cone. By taking schlieren photographs close to the instant of breakdown we have shown that, for the waxicon focus, breakdown occurred over the entire 8-cm schlieren field of view within the 50-ns ruby laser pulsewidth. At a later time, (1.3 μs) the effect of higher power density near the inner cone becomes apparent, since the radial shock velocity in the first few centimeters exceeds that for the plateau region of lower, constant power density. Other effects of slightly nonuniform intensity will be discussed later in this section.

In order to characterize the focused power density as a function of axial distance, the length of laser induced breakdown plasma was measured at different incident laser energies for each of three gases. Argon, air, and nitrogen were chosen for these experiments, since the optically induced breakdown thresholds for the first two have been accurately measured by other investigators.[20,21] The breakdown thresh-

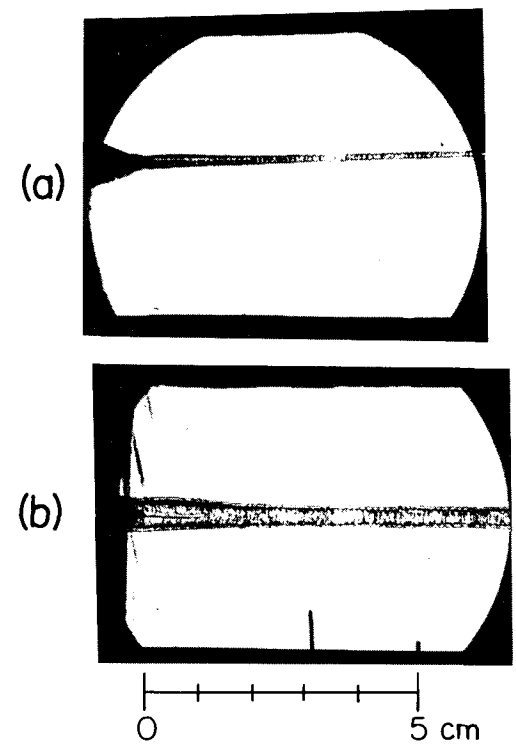

FIG. 4. Ruby laser schlieren photographs of laser induced breakdown plasmas in argon. (a) 0.3 μs after peak laser power; (b) 1.3 μs after peak laser power.

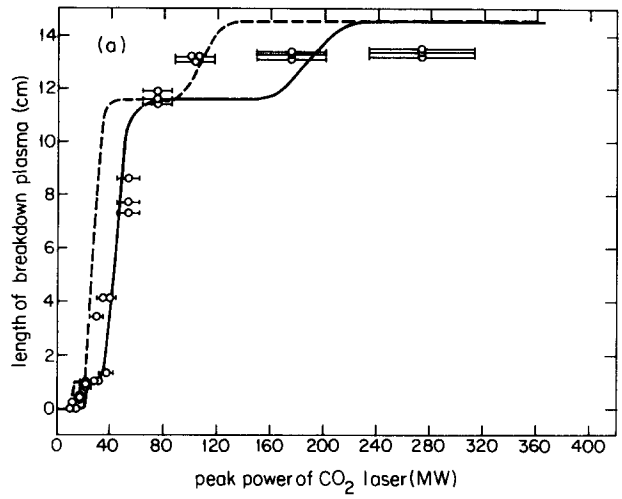

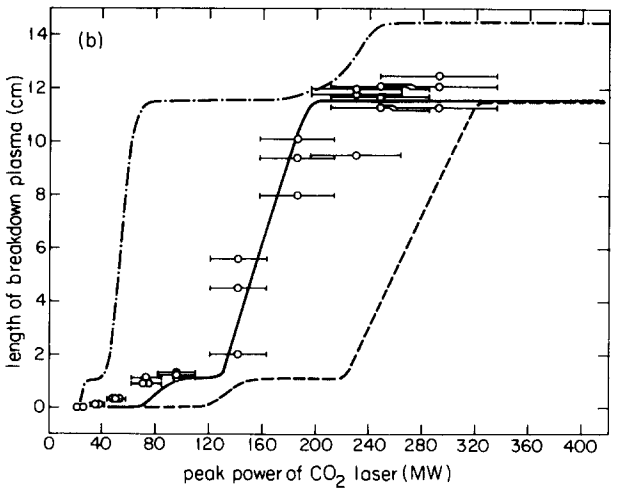

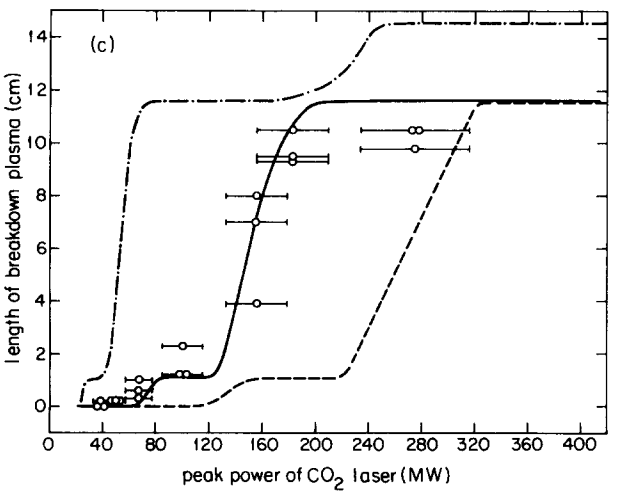

FIG. 5. Length of laser induced breakdown plasma from the waxicon focus as a function of peak incident laser power. Points represent experimental data, curves are from the ray tracing code. Solid curves were obtained using best fit thresholds. (a) Argon data. Dashed curve was obtained using code output with a tabulated breakdown threshold of 3×10^8 W/cm^2. (b) Air data. Dashed curve was obtained using code output with a tabulated breakdown threshold for highly filtered air of 3×10^9 W/cm^2. Dot–dashed curve was obtained using code output with tabulated breakdown threshold for unfiltered air of 6×10^8 W/cm^2. (c) N_2 data. Theoretical curves were obtained using the same breakdown thresholds as were used in the air experiment.[20]

old for nitrogen has been measured[20] to be the same as air within experimental error. These three gases also have important applications to channel dynamics research. For example, nitrogen is advantageous because its gas chemistry is much less complex than air. Research grade bottled gases flowed through the chamber in these experiments.

The experimental data points for these three gases are plotted in Fig. 5 along with theoretical curves obtained from the ray tracing code using tabulated breakdown thresholds. Data in Fig. 5(a) shows reasonable agreement with the breakdown lengths predicted from the ray tracing code using tabulated values of argon breakdown thresholds. Air and nitrogen breakdown data given in Fig. 5(b) and 5(c) lie within the range defined by tabulated values for unfiltered and highly filtered air and are identical to within experimental error. It should be noted that over a broad range of power levels the waxicon focus concentrated the laser energy in a fixed length of breakdown plasma in the plateau region of the intensity. This breakdown plasma always occurred at the same location, making it possible to vary the optical energy input to this given plasma length. This is an important characteristic of the waxicon for channel dynamics experiments. It should be noted that radical expansion can occur during the CO_2 laser pulse. Previous experiments have shown that, for conventional focusing systems, as the laser power is increased the region of breakdown moves axially toward the focusing element.[22]

Hot, reduced density channels are formed within the first 30 μs following energy deposition, when pressure equilibrium is reached between the inside and outside of the channel. Figure 6 represents a series of ruby laser schlieren photographs for channels generated by two techniques: (a) CO_2 laser induced breakdown or (b) laser guided electrical discharges in which the waxicon also functions as an electrode.

For the CO_2 laser induced channels shown in the left-hand column of Fig. 6, the radially propagating shock wave is clearly visible in the first two photographs. Of interest in the 13-μs schlieren photograph is the slight variation in the radial shock speed as a function of the axial position. This effect was reproducible and is believed to be caused by small nonuniformities in the optical energy deposition in the breakdown plasma which resulted from slight axial variations in the focused laser intensity. This intrepretation was supported by our observation that, close to the breakdown threshold, reproducible gaps in the breakdown plasma were observed. The source of this axial nonuniformity of intensity is believed to be periodic inaccuracies in the machining process. This effect could be eliminated by using optical grade machining. The effects of even slight differences in intensities on channel dynamics are seen in the later stages of channel evolution (200 and 500 μs), at which time the channel breaks up and mixing of hot channel gases with cold outside gases begins. Note that at these times the channel radius near the waxicon tip is largest. If one assumes pressure equilibrium, the ideal gas law predicts that the cross-sectional area of the channel is proportional to temperature. This again implies that the initial optical energy input was highest near the waxicon tip.

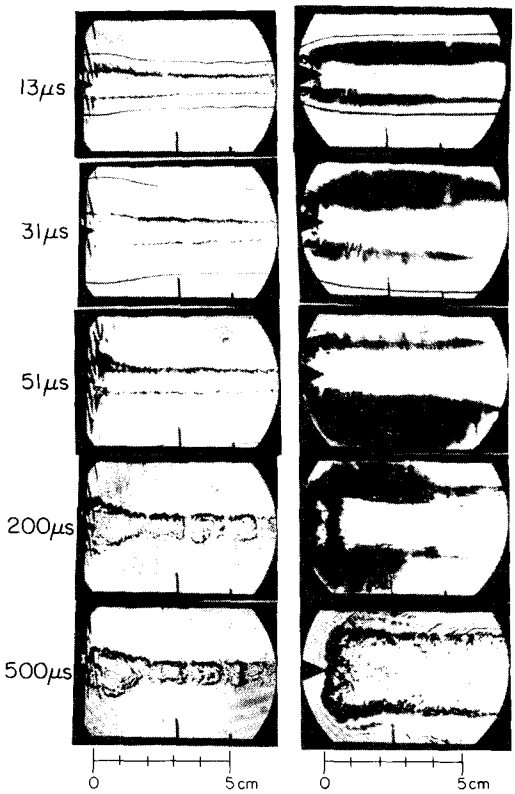

FIG. 6. Schlieren photographs of reduced density gas channels in argon. Channels in the left-hand side column were generated by laser induced breakdown alone using waxicon focus. Channels in the right-hand side column were generated by laser guided discharge using a focusing waxicon as an electrode. Times represent delay in microseconds between energy input to channel and ruby laser schlieren pulse.

Ohmic heating from the capacitor discharge gives laser guided discharges additional energy input over laser induced breakdown alone. The data of Fig. 6 (right column) shows this by the much larger shock velocity. Smooth, reduced density channels persist for more than 200 μs. Turbulent breakup begins at about 500 μs, but recognizable channels are still visibile at 900 μs.

ACKNOWLEDGMENTS

We gratefully acknowledge experimental assistance from J. E. Tucker and M. L. Brake. This research was supported by ONR Project 81-K-0700 and NSF Grant ECS-8105966. L. D. Horton is a postgraduate scholar under the Natural Sciences and Engineering Research Council of Canada.

[1]J. R. Greig, D. W. Koopman, R. F. Fernsler, R. E. Pechacek, I. M. Vitkovitsky, and A. W. Ali, Phys. Rev. Lett. **41**, 174 (1978).
[2]J. R. Greig, Bull. Am. Phys. Soc. **25**, 942 (1980).
[3]D. W. Koopman and K. A. Saum, J. Appl. Phys. **44**, 5328 (1973).
[4]J. M. Picone, J. P. Boris, J. R. Greig, M. Raleigh, and R. F. Fernsler, NRL Memorandum Report No. 4472, April 1981.
[5]G. Yonas, Sci. Am. **239**, 50 (1978).
[6]P. A. Miller, R. I. Butler, M. Cowan, J. R. Freeman, J. W. Poukey, T. P. Wright, and G. Yonas, Phys. Rev. Lett. **39**, 92 (1977).
[7]J. R. Freeman, L. Baker, and P. C. Cook, Nucl. Fusion **22**, 383 (1982).
[8]L. D. Horton and R. M. Gilgenbach, Phys. Fluids **25**, 1702 (1982).
[9]J. N. Olsen, J. Appl. Phys. **52**, 3279 (1981).
[10]J. N. Olsen and L. Baker, J. Appl. Phys. **52**, 3286 (1981).
[11]R. M. Measures, S. K. Wong, and P. G. Cardinal, J. Appl. Phys. **53**, 5541 (1982).
[12]D. P. Murphy, M. Raleigh, E. Laikin, J. R. Greig, and R. E. Pechacek, 9th International Symposium on Engineering Problems in Fusion Research, Chicago, 1981 (IEEE Publications, Piscataway, NJ, 1981), IEEE Cat. No. 81CH 1715-2 NPS, Vol. II, p. 1548.
[13]R. M. Gilgenbach, O. E. Ulrich, and L. D. Horton, Rev. Sci. Instrum. **54**, 109 (1983).
[14]A. Schmitt and R. S. B. Ong, J. Appl. Phys. **54**, 3003 (1983).
[15]H. Kleiman and R. W. O'Neil, Appl. Phys. Lett. **23**, 43 (1973).
[16]G. Weyl, J. Phys. D **12**, 33 (1979).
[17]J. M. Picone and J. P. Boris, Phys. Fluids **26**, 2 (1983).
[18]D. N. Mansell and T. T. Saito, Opt. Eng. **16**, 4 (1977).
[19]J. B. Arnold, R. E. Sladky, P. J. Steger, N. D. Woodall, and T. T. Saito, Opt. Eng. **16**, 4 (1977).
[20]D. C. Smith and R. G. Meyerand, *Laser Plasmas*, edited by G. Bekefi (Wiley, New York, 1976).
[21]D. E. Lencioni, Appl. Phys. Lett. **23**, 12 (1973).
[22]Yu. P. Raizer, *Laser Induced Discharge Phenomena* (Consultants Bureau, New York, 1977).